Electrochimica Acta 486 (2024) 144090

Contents lists available at ScienceDirect

Electrochimica Acta

journal homepage: www.journals.elsevier.com/electrochimica-acta

Composite anion exchange membranes based on graphene oxide for water electrolyzer applications

Nicholas Carboni [a], Lucia Mazzapioda [a], Angela Caprì [b], Irene Gatto [b], Alessandra Carbone [b], Vincenzo Baglio [b,*], Maria Assunta Navarra [a,c,*]

[a] Dipartimento di Chimica, Sapienza University of Rome, P.le Aldo Moro 5, Rome 00185, Italy
[b] Istituto di Tecnologie Avanzate per l'Energia "Nicola Giordano" (ITAE-CNR), Salita S. Lucia sopra Contesse 5, Messina 98126, Italy
[c] Hydro-Eco Research Center, Sapienza University of Rome, Via A. Scarpa 16, Rome 00161, Italy

ARTICLE INFO

Keywords:
Anion exchange membrane
Graphene oxide
Water electrolysis
Fumion
Alkaline Stability
Enhanced Performance

ABSTRACT

Anion Exchange Membrane Water Electrolyzers (AEMWE) hold the promise of combining the advantages of both liquid alkaline and PEM technologies, offering higher purity hydrogen production, improved efficiency, and dynamic behaviour. Nevertheless, AEM systems face notable challenges, particularly in enhancing the ion conductivity and stability of the membrane. The alkaline chemical stability of the AEMs is, in particular, one of the biggest issues, giving the high alkaline solutions used as electrolyte.

To overcome those problems, here in this work, the strategy chosen is the simple addition of an inorganic filler in the polymer matrix of the membrane. Various amounts of Graphene Oxide (GO), synthesized using the modified Hummers method, were incorporated into Fumion-based membranes. The resulting AEMs shows improved water uptake, chemical stability, thermal stability and, with the right amount of filler, also enhanced conductivity. In particular, all the composite membranes show diminished weight loss and I.E.C. loss after 170 h in 6 M KOH at 80 °C. The Fumion-GO AEM with 3 %GO (wt%) shows improved conductivity and a remarkable current density higher than 1 A/cm^2 at 2 V and 60 °C in the chronoamperometric test.

1. Introduction

Hydrogen has emerged as a highly promising vector for the storage and transportation of energy derived from renewable sources [1,2]. Its versatility and environmentally friendly characteristics make it a key player in the transition to a sustainable energy future. Hydrogen can be generated through various methods, including natural gas reforming, coal or biomass gasification, and electrolysis [3,4]. Among these methods, hydrogen production via water splitting using an electrolyzer stands out as one of the most environmentally friendly approaches. This is particularly true when renewable energy sources like wind or solar power are used to provide the electrical energy required for the electrolysis process. In such cases, hydrogen production becomes inherently "green" as it does not result in direct carbon emissions [5,6].

Liquid alkaline electrolysis stands out as one of the most mature and well-developed technologies in this context [7]. Its advantages lie in the potential for cost-effectiveness, largely due to the high pH environment that allows for the use of platinum group metal (PGM)-free catalysts [8,9]. However, it is not without its drawbacks, including relatively low current density due to the physical separation of electrodes and the unsatisfactory coupling with intermittent sources [10].

On the other hand, proton exchange membrane (PEM)-based systems represent a newer and more dynamic electrolysis technology. These systems involve electrodes in direct contact with a polymeric membrane to form a membrane-electrode assembly (MEA). The "zero-gap" approach, minimizing electrode distance and ohmic loss, has been crucial for improving their performance [11,12]. PEM electrolysis offers higher operating current density, enhanced efficiency, rapid response, fast start-up, and a broader operating range. It is favoured for its safety features and the potential to produce high-purity hydrogen even under high differential pressure conditions. However, the use of PGM catalysts and expensive membranes (e.g. Nafion) increases the cost of the devices [13].

In contrast, anion exchange membrane (AEM) electrolyzers, while less commercially established, share similarities with both liquid alkaline and PEM electrolysis technologies [14]. Like PEM systems, AEM

* Corresponding authors.
E-mail addresses: vincenzo.baglio@itae.cnr.it (V. Baglio), mariassunta.navarra@uniroma1.it (M.A. Navarra).

https://doi.org/10.1016/j.electacta.2024.144090
Received 29 January 2024; Received in revised form 8 March 2024; Accepted 9 March 2024
Available online 11 March 2024

electrolyzers employ a zero-gap approach, but the key distinction lies in the membrane's ability to conduct hydroxide ions [15]. AEM electrolyzers hold the promise of combining the advantages of both liquid alkaline and PEM technologies, offering higher purity hydrogen production, improved efficiency, and dynamic behaviour [16]. Nevertheless, AEM systems face notable challenges, particularly in enhancing the ion conductivity and stability of the membrane [14]. The alkaline chemical stability of the AEMs is, in particular, one of the biggest issues, giving the high alkaline solutions used as electrolyte [17,18].

To overcome those problems, here in this work, the strategy chosen is the simple addition of an inorganic filler in the polymer matrix of the membrane. Various amounts of Graphene Oxide (GO) were incorporated into the Fumion® FAA-3 ionomer. These solutions were then used to fabricate AEMs by the solvent casting method to obtain composite membranes with GO as filler. GO was synthesized using the modified Hummers Method [19]. Morphological and structural characterizations of the additive and the membranes were carried out using various techniques, together with the electrochemical investigations in a 5 cm^2 single electrolysis cell.

Among the various nanomaterial fillers available, graphene oxide (GO) has received substantial attention due to its remarkable thermal stability and high specific surface area [20,21]. Despite extensive research efforts focused on enhancing the performances of commercial PEMs like Nafion through the addition of nanomaterials for fuel cell and water electrolyzer applications, there exists a noticeable gap in the study of enhancing commercial AEMs (e.g., Fumion, Sustainion, Aemion) via GO incorporation. Very recently Arunkumar et al.[22] showed that unfunctionalized GO can be useful to improve the performances of AEMs in fuel cells and here in this work we further explore the potentialities of GO, trying different compositions and testing the membranes for hydrogen production, using a single 5 cm^2 electrolysis cell. Graphene oxide, in fact, enhances OH^- ion conductivity through the Grotthuss mechanism, involving the breaking and reformation of hydrogen bonds, along with the adsorption of water molecules on the GO surface [23]. Furthermore, the interaction between the oxygen-containing groups in GO and the polymer matrix may enhance membrane stability, reducing OH^- activity against the electropositive carbon backbone and conductive groups [24].

Despite its cost-effectiveness, Fumion exhibits limitations in terms of physicochemical stability and electrochemical performance, particularly when compared to other commercial AEM materials [25]. Fumion is widely used as an electrolyte/ionomer in various energy storage and conversion devices, including fuel cells, water and CO_2 electrolyzers, and flow batteries. Its affordability has made it a popular choice for evaluating electrocatalyst performance in membrane-based electrochemical devices [26–28]. Consequently, there is a compelling need to enhance Fumion properties through chemical modification, and the incorporation of functional fillers/polymers into the Fumion membrane is an interesting approach that can also be used with other polymeric AEMs [29–31].

Hence the present study adopts a straightforward and cost-effective approach, focusing on enhancing Fumion membranes by incorporating GO in the polymeric matrix. This research focuses on the effects of GO addition on various properties of Fumion including morphological, ion conductivity, thermal stability, and chemical stability properties. Additionally, it investigates single-cell performance and compares the results with a pristine Fumion membrane prepared without the addition of GO. This study demonstrated the positive impact of introducing graphene oxide into Fumion membranes: the right amount can enhance performances respect to the pristine AEM, particularly in terms of physicochemical stability and hydroxide ion conductivity. To the best of our knowledge, this is the first paper that investigates the role of the addition of high GO content in the Fumion membrane (> 1.5 % in weight with respect to polymer) and the behavior of Fumion-GO composite membranes for water electrolyzer applications.

2. Experimental methods

2.1. Materials

Fumasep® FAA3–50 membrane, FAA3 shredded film and FAA-3-SOLUT-10 ionomer were bought from FuMa-Tech. Potassium Permanganate ($KMnO_4$), Hydrogen Peroxide (H_2O_2) and Potassium Hydroxide (KOH) were bought from Sigma-Aldrich. Graphite (TIMREX HSAG300) was bought from TIMCAL and concentrated Sulphuric Acid 96 % (H_2SO_4), Ethanol (96 %) and n-propanol (99.5 %) was bought from Carlo Erba.

2.2. GO synthesis

Graphene Oxide was synthesized using the modified Hummers method [19]. Graphite powder was mixed with concentrated H_2SO_4 (solid to liquid ratio 1:24). $KMnO_4$ (3:1 in weight respect to graphite) was carefully added to the mixture in an ice bath and then the temperature was raised to 40 °C for 30 min. Then after the addition of distilled water the temperature was set to 95 °C for another 30 min. H_2O_2 (30 % in wt) was then added to the mixture (1:5 solid to liquid with respect to graphite). The precipitate was washed and then dispersed in water for sonication and centrifugation. The supernatant was separated from the precipitate and let evaporate to obtain GO.

2.3. Membrane preparation

The composite membranes were prepared by a simple solution casting method [32] by adding various amounts of GO (3 %, 5 % and 7 % in weight with respect to polymer) to the ionomer solution (FAA-3--SOLUT-10) and stirring for one night. These solutions were then cast in a petri dish and dried in an oven at 80 °C for 24 h. The resulting membranes were then stored dry in the brominated form and activated in 1 M KOH before the tests. The pristine Fumion membrane was prepared with the same procedure without the addition of GO and named Fumion Recast.

For all the tests the measure was repeated at least two times.

2.4. Membrane-electrode-assembly (MEA) preparation and electrochemical characterization

The anode electrode consisted of a Ni felt (Bekipor ST Sintered metal fibre matrix, type 2Ni06–020, Bekaert) to act as the catalyst, diffusion layer and current collector. The cathodic electrode was prepared as reported in [33], using a commercial 40 % Pt/C (Alfa Aesar), with a Pt loading of 0.5 mg cm^{-2}, and a 20 wt.% of FAA3 ionomer (obtained starting from FAA3-shredded Fumatech film as reported in [34]) onto a Sigracet 25-BC Gas Diffusion Layer (SGL Carbon). The electrodes' geometrical area measured 5 cm^2. A membrane-electrode assembly (MEA) was prepared by cold-assembling the anode and cathode electrodes to the membrane. The cathode and membrane had been exchanged for 24 h in 1 M KOH aqueous solution at 25 °C prior to assembly. The electrochemical characterizations (polarization curves and chronoamperometry tests) were carried out in 5 cm^2 single-cell configuration using a potentiostat-galvanostat device PGSTAT302N (Autolab) at 60 °C and atmospheric pressure. I–V curves were performed at a scan rate of 5 mV/s and chronoamperometry tests were performed at 2 V. A 1 M KOH solution was fed at a flow rate of 5 ml/min by a peristaltic pump to the anode side.

The through-plane conductivity was measured by the Electrochemical Impedance Spectroscopy (E.I.S.), performed using a VSP potentiostat (BioLogic) at different temperatures (30–60 °C) from 100 kHz to 1 Hz with an amplitude of 10 mV. EL-CELL ECC-Std was used to perform the tests. The cell was assembled placing the membranes between two stainless steel disks and adding 60 µl of 1 M KOH solution. The membranes were exchanged in 1 M KOH solution for 24 h and then

cut in disks (10 mm diameter)

From the resistance values (intercept with the real part of the impedance in Nyquist plot) it is possible to calculate the conductivity of the membrane using the following relation:

$$\sigma = \frac{L}{RS}$$

Where σ is the conductivity, L is the thickness and S is the geometrical area of the of the membranes.

The in-plane OH^- conductivity was measured by a four-electrode method by using the Bekktech cell, as reported elsewhere [34]. The measurements were carried out in the range of temperature 30–60 °C, flowing humidified N_2 (100%RH). The E.I.S. parameters for the measurement were: 100 KHz - 1 Hz of frequency range and 50 mV of amplitude.

2.5. Ionic exchange capacity (I.E.C)

The Ionic Exchange Capacity was determined by titration, using a standardized 0.01 M HCl solution. The membranes were immersed in KOH for 24 h to exchange Br^- with OH^- and then immersed in 1 M NaCl solution for 24 h to substitute OH^- with Cl^-. The OH^- in solution was then determined by titration using Methyl Red as indicator. The I.E.C. was calculated using the following equation:

$$I.E.C. = \frac{M_{HCl} \times V_{HCl}}{m_{dry}}$$

Were m_{dry} is the weight of the membrane after 2 h under vacuum at 60 °C.

2.6. Water uptake (W.U.)

The W.U. is calculated using the following equation:

$$W.U.\ (\%) = \frac{m_{wet} - m_{dry}}{m_{dry}} \cdot 100$$

Were m_{dry} is the weight of the membrane after 2 h under vacuum at 60 °C and m_{wet} is the weight after 24 h in KOH at 20 °C.

2.7. Alkaline stability test

The alkaline durability test was performed by dipping the membrane in KOH 6 M at 80 °C for 170 h. The degradation was evaluated by weighting the membrane (after 2 h of drying under vacuum at 60 °C) and measuring the I.E.C. before and after the test.

2.8. Materials characterization

The samples were characterized using the following techniques:

Attenuated Total Reflectance - Fourier Transform Infrared (ATR-FTIR) analysis was carried out using a Bruker LUMOS II FTIR microspectrometer in reflection mode, recording 2048 scans for each sample at ambient temperature in the range of 400–4000cm^{-1}.

Raman spectra were acquired with a DILOR LabRam confocal micro-Raman with a He−Ne laser source at 632.7nm.

Scanning electron micrographs have been recorded by using a field emission scanning electron microscope (FESEM) at the CNIS research centre (ZEISS Auriga) equipped with an **energy-dispersive X-ray** probe (EDX) for the elemental analysis of samples. Giving the non-conductive nature of the membranes, a sputter coating with chromium (~10 nm) was done before the analysis.

Thermogravimetric Analysis (TGA) was performed under nitrogen flow from 25 °C to 700 °C with a heating rate of 10 °C min^{-1} (Mettler-Toledo TGA2, Mettler-Toledo, Columbus, OH, USA).

3. Results and discussion

3.1. Graphene oxide characterization

To be sure that the synthesis was successful, Graphene Oxide was characterized using Raman, ATR-FTIR, SEM and EDX.

The SEM micrographs and EDX table of the synthesized Graphene Oxide are shown in Fig. 1.

The SEM micrographs show the typical surface of GO, in which a thin, crumpled layered structure can be observed. The EDX analysis confirm the expected C/O ratio [19,35,36] that is near 3 ($C/O = 2{,}73$).

The IR and Raman analyses in Fig. 2 confirm the composition of the GO. In particular IR spectrum shows the signals of the characteristic peaks of the GO functionalities confirming the presence on the surface of O–H stretching (~3400 cm^{-1}) and bending (~1380 cm^{-1}), C = O stretching (~1700 cm^{-1}), C = C stretching (~1600 cm^{-1}), C–O stretching (~1260 cm^{-1}) and C–O–C stretching (~1080 cm^{-1}) vibrations [37].

Raman analysis shows the presence of the characteristic bands of carbon: D band around 1340 cm^{-1}, that arises from the breathing mode of aromatic rings and is only visible in the presence of disorder in the structure and G band around 1600 cm^{-1} related to the in-phase vibration of the graphite lattice [38,39]. The large I_D/I_G ratio of 2,97 indicates lattice defects in GO that may be attributed to the existence of different nature and amount of oxygenated functionalities, holes or permanent vacancies and extent of reorganization of carbon framework in its architecture [40]. The 2D band around 2700 cm^{-1} is the overtone of the D band [41]: it has very low intensity, it is very wide and is centred at lower Raman Shift (2680 cm^{-1}), suggesting the successfully exfoliation of GO sheets [42,43].

3.2. Composite membranes characterization and cell performance

Composite membranes were characterized and compared to the Fumion Recast AEM: Thickness, I.E.C, W.U., morphology, alkaline stability, thermal degradation and conductivity were investigated, along with in cell tests (polarizations and chronoamperometry). The appearance of the prepared membranes is reported in Fig. 3, showing a good dispersion of the GO additive on a macro scale.

3.2.1. Thickness, ionic exchange capacity and water uptake

It is possible to see from Table 1 that the studied AEMs have all comparable thickness. The I.E.C values are very similar between each other, because Graphene Oxide does not contain OH^- exchanging groups. The small increasing of I.E.C with GO content is attributed to the adsorption of KOH solution that can be measured by titration but do not participate to the conduction. The W.U. increases proportionally to the amount of GO and is attributed to its high hygroscopicity [21].

3.2.2. Surface morphology

Fig. 4 shows the SEM micrographs of the surface of the composite membranes along with the Fumion Recast. The surface roughness and inhomogeneity increase proportionally to the GO content: 3 % GO shows a relatively smooth surface, not so different from the Fumion Recast, while 7 % GO shows Graphene Oxide deposits on the surface and high inhomogeneity due to excessive filler content.

3.2.3. Thermogravimetric analysis

Thermogravimetric analysis (Fig. 5) shows the thermal stability of the graphene oxide, Fumion recast and the composite membranes. Three different regions are observed, the first (25–150 °C) is attributed to the water desorption from the samples, the second (150–400 °C) is related to the decomposition of the GO and polymer functional groups and the last mass loss (>400 °C) is caused by the decomposition of the polymeric backbone [44].

The peak of the first derivative indicates the point of greatest rate of change on the weight loss curve and it is correlated to the thermal

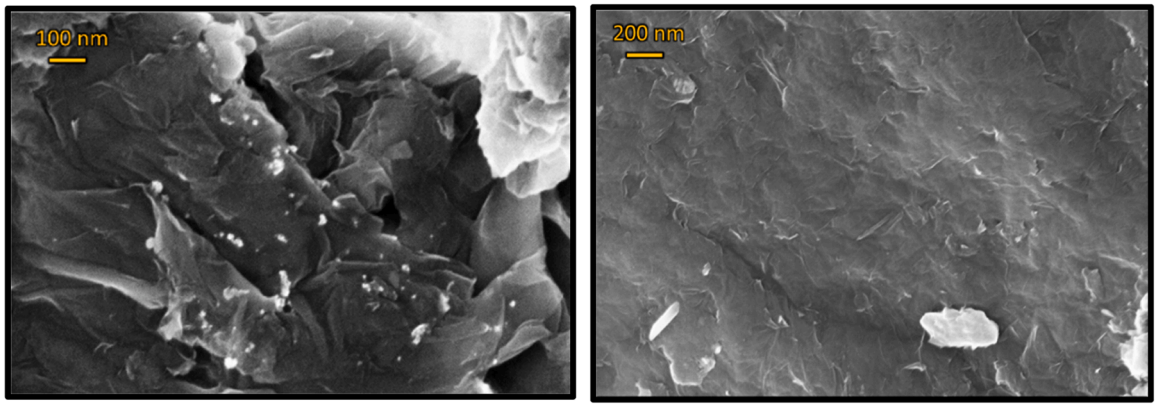

a)

b)

EDX Analysis	
Element	**Atomic %**
C	70.7
O	25.9
N, Na, S, Mg, K (impurities)	3.4

Fig. 1. SEM micrographs of the synthesized GO at different magnifications (a) 200 K X and (b) 100 K X and table of EDX analysis.

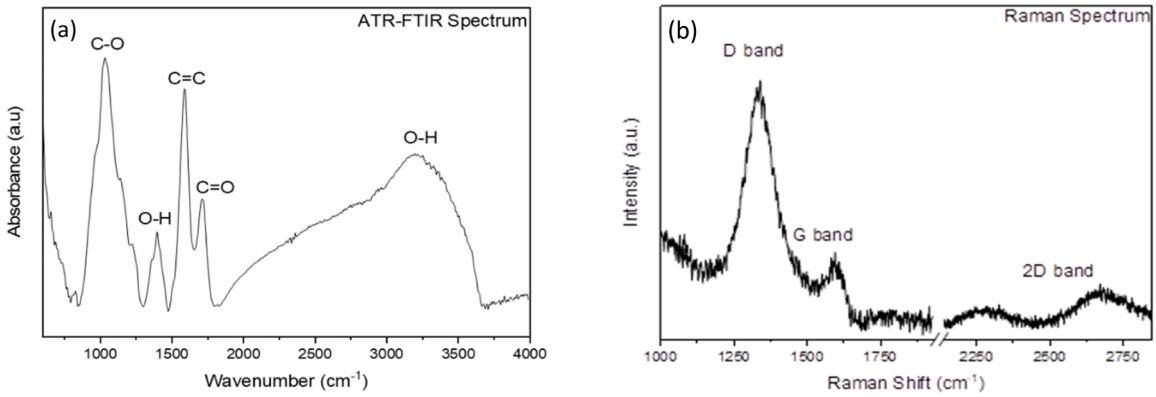

Fig. 2. (a) ATR-FTIR spectrum of GO. (b) Raman Spectrum of GO.

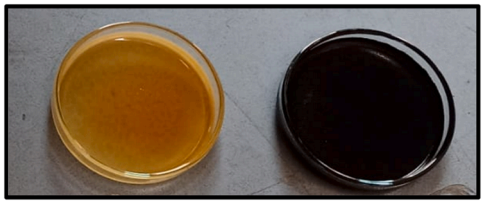

Fig. 3. Image of the Fumion Recast (left) and 7 % GO (right) prepared membranes.

stability [45]: GO composite membranes shows shifts at slightly higher temperatures (~ 5 °C for the peaks around 330 °C and ~ 2 °C for the ones around 415 °C), suggesting favourable interactions between the filler and the polymer that enhance the thermal stability of the polymer functional groups and backbone. Moreover, all the composite membranes show more residual weight respect to the Fumion recast, indicating less degree of degradation.

Table 1
Thickness, I.E.C and W.U. of the studied membranes.

Membrane	Thickness (μm)	I.E.C (meq/g)	W.U. (%)
Fumion Recast	62.3 ± 4.1	1.09 ± 0.03	18.46 ± 2.7
3 % GO	59.7 ± 7.1	1.12± 0.02	36.31 ± 3.1
5 % GO	86 ± 2.8	1.14± 0.01	44.11 ± 5.3
7 % GO	69.7 ± 1.9	1.15± 0.01	61.49 ± 8.0

3.2.4. *Alkaline stability*

The alkaline durability test was performed by dipping the membrane in 6 M KOH at 80 °C for 170 h and confirm the positive effects of the GO inclusion in the membranes. All the composite membranes show less I.E.C. and weight loss compared to the Fumion Recast (see Table 2): this is attributed to the electrostatic interactions and hydrogen bonding of the functional groups of the additive with the polymer, which can diminish the OH^- attack on both the cationic groups and the polymeric backbone. Increasing GO content leads to more interactions, resulting in a high alkaline stability (Table 2).

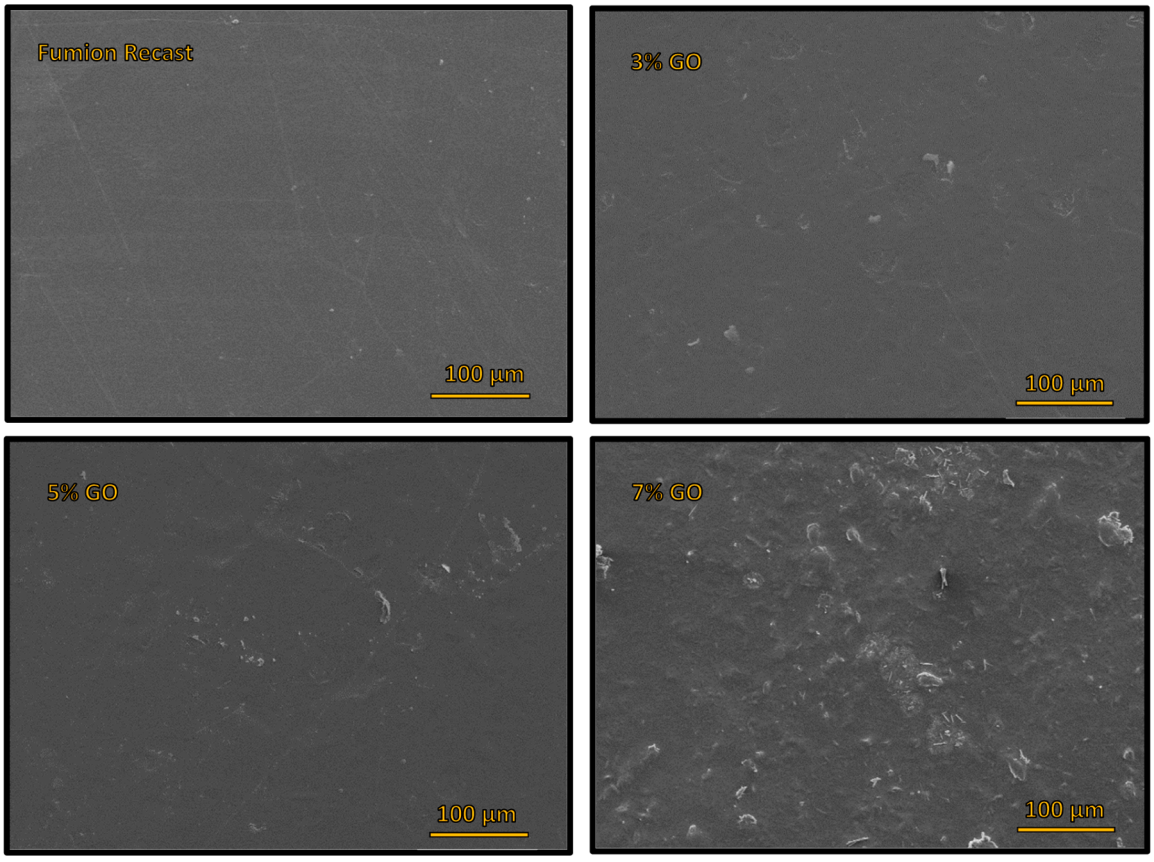

Fig. 4. SEM micrographs of the pristine Fumion Recast along with the composite membranes.

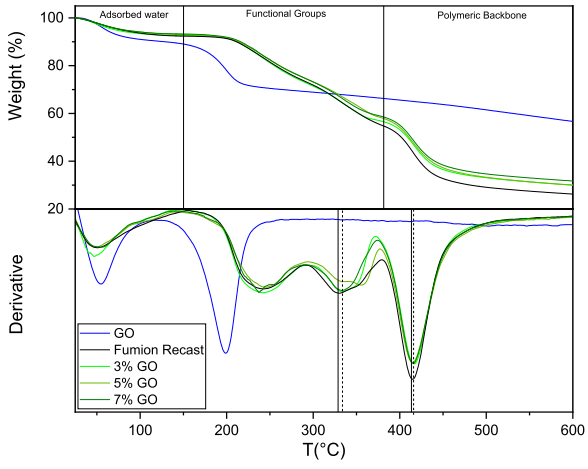

Fig. 5. TGA and the derivative of the curves of Graphene Oxide along with the studied membranes. The black lines in the bottom graph are in correspondence of the Fumion recast derivative peak (solid line) and the composite membranes derivative peak (dash line). The heating rate is 10 °C/min.

Table 2
Percentile weight loss and I.E.C. loss of the studied membranes.

Membrane	Weight loss (%)	I.E.C loss (%)
Fumion Recast	30.13 ± 3.1	89.9 ± 0.05
3 % GO	10.75 ± 2.3	83.3 ± 0.02
5 % GO	8.52 ± 1.7	82.4 ± 0.04
7 % GO	8.33 ± 2.0	76.5 ± 0.03

3.2.5. *Through-Plane conductivity*

The comparison of the through-plane conductivity obtained from E.I.S. for the studied samples is reported in Fig. 6. For all membranes, as expected, the conductivity increases with the increase of temperature. The trend follows the one observed in the chronopotentiometry tests as well as the performance in terms of polarization curves, with the 3 % GO having the highest conductivity of the studied AEMs, while the lowest values were found for 5 % and 7 % composite membranes, due to the high content of GO introduced in the polymeric matrix. For selected membranes also in-plane conductivity tests were conducted (Figure S1

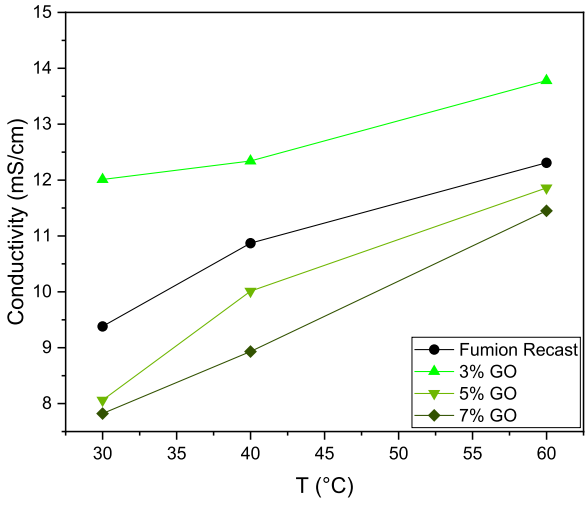

Fig. 6. Comparison of through plane conductivity in the temperature range 30–60 °C calculated from E.I.S.

of the supporting information), resulting in good agreement with the through-plane conductivity tests.

The OH^- conductivity, in the temperature range 30–60 °C, shows an Arrhenius behaviour; thus, the activation energy can be determined. Table 3 shows the activation energies of the studied samples: 3 % GO shows the lowest activation energy, about half the one of Fumion Recast, indicating favoured OH^-transport, and it is in accordance with the highest conductivity values and single cell performance (next section).

3.2.6. Polarization curves

Fig. 7 shows the polarization curves of the studied membranes. The composite membrane with 3 % GO has the best performance, becoming even better at high potentials, confirming that the addition of Graphene Oxide boosts the conductivity, decreasing the water splitting overpotential. These results are significantly better than those obtained with a commercial FAA3–50 membrane previously investigated [33]. Increasing the GO content the performances decrease, probably due to the excessive interaction between GO and cationic groups of the polymer, and formation of clusters, that can hinder the hydroxide transport.

3.2.7. Chronoamperometric tests

The chronoamperometric tests were used to investigate the stability of the membrane over time and compare the behaviour of the composite materials with respect to the pristine Fumion Recast, used as the reference. The tests were conducted at 2 V for about 15–20 h feeding 1 M KOH solution. The results are reported in Fig. 8. These studies do not represent a durability test, since at least 1000 h would be necessary to evaluate the stability of the different components, including the membranes. Here, the tests were performed to investigate the different behavior of the membranes subjected to steady-state experiments, not dynamic ones, as in the case of J-V curves recorded at a scan rate of 5 mV s^{-1}. The curve's behaviour over time is consistent with that reported in earlier studies [46,47] wherein there is an initial drop in current density, probably caused by the CO_2 from the environment that can form carbonates, which can initially poison the electrodes as well as the membrane. Moreover, there are other possible explanations for this phenomenon, such as membrane degradation or poisoning, catalyst deactivation, electrode constraints (flooded electrode with oxygen bubble removal limitations), etc.

As observed in Fig. 8, all the composite membranes have good performances in terms of current density even in this test. The loss in performance is evaluated by calculating the drop in current density over the time of the test and with respect to the starting current density value. The 3 % GO in particular shows high performances, outperforming Fumion Recast and maintaining a current density higher than 1 A/cm^2 for all the time of the test. 3 % GO shows also a significant reduction of J drop with respect to the pristine AEM.

Those tests confirm that increasing the content of GO in the membrane has a negative effect on the performance. This might be because an increase in GO content in the polymer matrix may reduce the mobility of the ions via aggregations and block the transport pathways for hydroxide ions through the membrane, reducing the conductivity and the stabilization effect. It is also possible that excessive interaction between GO groups and the cationic groups of the Fumion can hinder OH^- mobility. The differences in the stability trend respect to the alkaline stability test it attributed to the inhomogeneity of the membrane with the increase of GO content, that can lead to mechanical degradation and interfacial failure between AEM and electrode, leading to High Frequency Resistance (HFR) increase and performance loss [17,48]. It is also worth noting that, as stated above, at least 1000 h would be necessary to appreciate the stability of the membranes, so it is possible that in the long term the trend can change.

Table 3
Activation Energies for the OH^- conduction of the studied membranes obtained from E.I.S measurement.

Membrane	Eact, kJ/mol
Fumion Recast	7.34
3 % GO	3.96
5 % GO	10.39
7 % GO	10.69

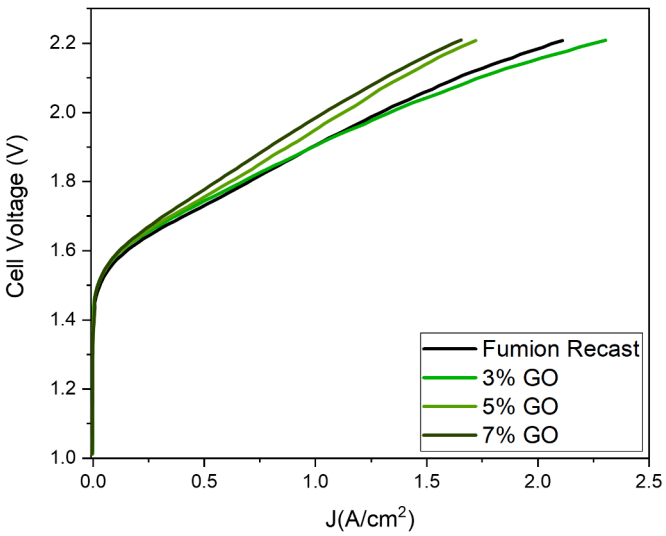

Fig. 7. Polarization curves of the composite membranes compared to the Fumion recast, for all the samples linear sweep voltammetries were performed at a scan rate of 5 mV/s at 60 °C.

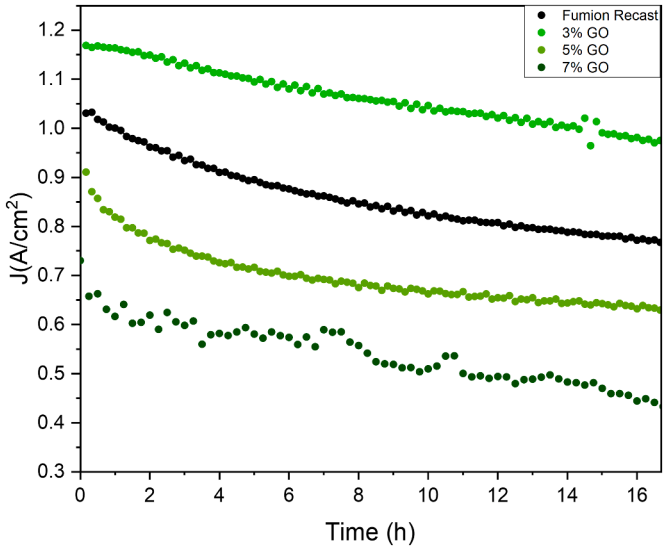

Fig. 8. Chronoamperometry tests of the composite membranes compared to the pristine Fumion Recast and table of the current density drops for each membrane.

4. Conclusion

Here in this work, we have explored the potentialities of Graphene Oxide in Fumion-based AEMs for water electrolyzer applications, developing cost-effective AEMs with improved water uptake, chemical stability, thermal stability and, with the right amount of filler, also enhanced conductivity. As stated above one of the major problems regarding AEMs is the chemical stability in alkaline environment and we demonstrate the effectiveness of the simple addition of GO in the AEMs polymer matrix: all the composite membranes have, in fact, diminished

weight loss and I.E.C. loss after 170 h in KOH 6 M at 80 °C. In this case more GO in the membrane help the stability, resulting in the 7 % GO AEM as the most stable in alkaline environment. For what concern the conductivity and in cell tests, the trend seems to be the opposite and increasing the GO content leads to inhomogeneities and aggregation, resulting in 3 % GO AEM as the most performing one, outperforming also the pristine Fumion Recast and maintaining a current density higher than 1 A/cm^2 in the chronopotentiometry test. A compromise between stability and conductivity is therefore needed and optimizing the membrane fabrication to obtain high homogeneous AEMs can be critical for those type of systems. 5 % GO AEM is also interesting, as it has high alkaline stability and is not as inhomogeneous as the 7 % GO AEM: achieving a better filler dispersion can be a viable strategy to improve the electrochemical performances while maintaining the high chemical stability.

CRediT authorship contribution statement

Nicholas Carboni: Writing – original draft, Investigation, Data curation. **Lucia Mazzapioda:** Formal analysis. **Angela Caprì:** Investigation, Data curation. **Irene Gatto:** Supervision, Methodology. **Alessandra Carbone:** Writing – review & editing, Investigation, Data curation. **Vincenzo Baglio:** Writing – review & editing, Supervision, Project administration, Conceptualization. **Maria Assunta Navarra:** Writing – review & editing, Supervision, Conceptualization.

Declaration of competing interest

The authors declare that they have no known competing financial interests or personal relationships that could have appeared to influence the work reported in this paper.

Data availability

Data will be made available on request.

Acknowledgments

The authors thank the Italian Ministry of University and Research (MUR) for funding through the FISR2019 project AMPERE (FISR2019_01294).

Supplementary materials

Supplementary material associated with this article can be found, in the online version, at doi:10.1016/j.electacta.2024.144090.

References

[1] J.R. Varcoe, P. Atanassov, D.R. Dekel, A.M. Herring, M.A. Hickner, Paul.A. Kohl, A. R. Kucernak, W.E. Mustain, K. Nijmeijer, K. Scott, T. Xu, L. Zhuang, Anion-exchange membranes in electrochemical energy systems, Energy Environ. Sci. 7 (2014) 3135–3191, https://doi.org/10.1039/C4EE01303D.

[2] N. Du, C. Roy, R. Peach, M. Turnbull, S. Thiele, C. Bock, Anion-Exchange membrane water electrolyzers, Chem. Rev. 122 (2022) 11830–11895, https://doi.org/10.1021/acs.chemrev.1c00854.

[3] H. Ishaq, I. Dincer, C. Crawford, A review on hydrogen production and utilization: challenges and opportunities, Int. J. Hydrogen Energy 47 (2022) 26238–26264, https://doi.org/10.1016/j.ijhydene.2021.11.149.

[4] P. Nikolaidis, A. Poullikkas, A comparative overview of hydrogen production processes, Renew. Sustainable Energy Rev. 67 (2017) 597–611, https://doi.org/10.1016/j.rser.2016.09.044.

[5] A. Patonia, R. Poudineh, Cost-competitive Green hydrogen: How to Lower the Cost of Electrolysers? Oxford Institute for Energy Studies, 2022.

[6] S. Shiva Kumar, H. Lim, An overview of water electrolysis technologies for green hydrogen production, Energy Reports 8 (2022) 13793–13813, https://doi.org/10.1016/j.egyr.2022.10.127.

[7] J.C. Ehlers, A.A. Feidenhans'l, K.T. Therkildsen, G.O. Larrazábal, Affordable green hydrogen from alkaline water electrolysis: key research needs from an industrial perspective, ACS Energy Lett. 8 (2023) 1502–1509, https://doi.org/10.1021/acsenergylett.2c02897.

[8] J. Brauns, T. Turek, Alkaline water electrolysis powered by renewable energy: a review, Processes 8 (2020) 248, https://doi.org/10.3390/pr8020248.

[9] C. Alegre, C. Busacca, A. Di Blasi, O. Di Blasi, A.S. Aricò, V. Antonucci, E. Modica, V. Baglio, Electrospun carbon nanofibers loaded with spinel-type cobalt oxide as bifunctional catalysts for enhanced oxygen electrocatalysis, J. Energy Storage 23 (2019) 269–277, https://doi.org/10.1016/j.est.2019.04.001.

[10] A. Abdel Haleem, J. Huyan, K. Nagasawa, Y. Kuroda, Y. Nishiki, A. Kato, T. Nakai, T. Araki, S. Mitsushima, Effects of operation and shutdown parameters and electrode materials on the reverse current phenomenon in alkaline water analyzers, J. Power Sources 535 (2022) 231454, https://doi.org/10.1016/j.jpowsour.2022.231454.

[11] S. Siracusano, V. Baglio, A. Stassi, L. Merlo, E. Moukheiber, A.S. Arico′, Performance analysis of short-side-chain Aquivion® perfluorosulfonic acid polymer for proton exchange membrane water electrolysis, J. Memb. Sci. 466 (2014) 1–7, https://doi.org/10.1016/j.memsci.2014.04.030.

[12] X. Sun, S. Simonsen, T. Norby, A. Chatzitakis, Composite membranes for high temperature PEM fuel cells and electrolysers: a critical review, Membranes (Basel) 9 (2019) 83, https://doi.org/10.3390/membranes9070083.

[13] C. Li, J.B. Baek, The promise of hydrogen production from alkaline anion exchange membrane electrolyzers, Nano Energy 87 (2021) 106162, https://doi.org/10.1016/j.nanoen.2021.106162.

[14] R. Vinodh, S.S. Kalanur, S.K. Natarajan, B.G. Pollet, Recent advancements of polymeric membranes in Anion Exchange Membrane Water Electrolyzer (AEMWE): a critical review, Polymers 15 (2023) 2144, https://doi.org/10.3390/polym15092144.

[15] T. Lim, S.K. Kim, Non-precious hydrogen evolution reaction catalysts: stepping forward to practical polymer electrolyte membrane-based zero-gap water electrolyzers, Chem. Eng. J. 433 (2022) 133681, https://doi.org/10.1016/j.cej.2021.133681.

[16] P. Shirvanian, A. Loh, S. Sluijter, X. Li, Novel components in anion exchange membrane water electrolyzers (AEMWE's): status, challenges and future needs. A mini review, Electrochem. Commun. 132 (2021) 107140, https://doi.org/10.1016/j.elecom.2021.107140.

[17] W.E. Mustain, M. Chatenet, M. Page, Y.S. Kim, Durability challenges of anion exchange membrane fuel cells, Energy Environ. Sci. 13 (2020) 2805–2838, https://doi.org/10.1039/D0EE01133A.

[18] D. Li, A.R. Motz, C. Bae, C. Fujimoto, G. Yang, F.Y. Zhang, K.E. Ayers, Y.S. Kim, Durability of anion exchange membrane water electrolyzers, Energy Environ. Sci. 14 (2021) 3393–3419, https://doi.org/10.1039/D0EE04086J.

[19] J. Chen, B. Yao, C. Li, G. Shi, An improved Hummers method for eco-friendly synthesis of graphene oxide, Carbon 64 (2013) 225–229, https://doi.org/10.1016/j.carbon.2013.07.055.

[20] Y.C. An, X.X. Gao, W.L. Jiang, J.L. Han, Y. Ye, T.M. Chen, R.Y. Ren, J.H. Zhang, B. Liang, Z.L. Li, A.J. Wang, N.Q. Ren, A critical review on graphene oxide membrane for industrial wastewater treatment, Environ. Res. 223 (2023) 115409, https://doi.org/10.1016/j.envres.2023.115409.

[21] D. Chen, H. Feng, J. Li, Graphene oxide: preparation, functionalization, and electrochemical applications, Chem. Rev. 112 (2012) 6027–6053, https://doi.org/10.1021/cr300115g.

[22] I. Arunkumar, A.R. Kim, S.H. Lee, D.J. Yoo, Enhanced fumion nanocomposite membranes embedded with graphene oxide as a promising anion exchange membrane for fuel cell application, Int. J. Hydrogen Energy 52 (2024) 139–153, https://doi.org/10.1016/j.ijhydene.2022.10.184.

[23] M. Fukuda, Md.S. Islam, Y. Shudo, J. Yagyu, L.F. Lindoy, S. Hayami, Ion conduction switching between H^+ and OH^- induced by pH in graphene oxide, Chem. Commun. 56 (2020) 4364–4367, https://doi.org/10.1039/D0CC00769B.

[24] O. Movil, L. Frank, J.A. Staser, Graphene oxide–polymer nanocomposite anion-exchange membranes, J. Electrochem. Soc. 162 (2015) F419–F426, https://doi.org/10.1149/2.0681504jes.

[25] W. Ng, W. Wong, N. Rosli, K. Loh, Commercial Anion Exchange Membranes (AEMs) for fuel cell and water electrolyzer applications: performance, durability, and materials advancement, Separations 10 (2023) 424, https://doi.org/10.3390/separations10080424.

[26] I. Arunkumar, R. Gokulapriyan, V. Sakthivel, A.R. Kim, M.S. Oh, J.Y. Lee, S. Kim, S. Lee, D.J. Yoo, Functionalized graphene nanofiber-incorporated fumion anion-exchange membranes with enhanced alkaline stability and fuel-cell performances, ACS Appl Energy Mater 6 (2023) 7702–7713, https://doi.org/10.1021/acsaem.3c01182.

[27] M. Liu, H. Hu, Y. Kong, I.Z. Montiel, V. Kolivoška, A.V. Rudnev, Y. Hou, R. Erni, S. Vesztergom, P. Broekmann, The role of ionomers in the electrolyte management of zero-gap MEA-based CO_2 electrolysers: a Fumion vs. Nafion comparison, Appl. Catal. B 335 (2023) 122885, https://doi.org/10.1016/j.apcatb.2023.122885.

[28] M.T. Tsehaye, X. Yang, T. Janoschka, M.D. Hager, U.S. Schubert, E. Planes, F. Alloin, C. Iojoiu, Anion exchange membranes with high power density and energy efficiency for aqueous organic redox flow batteries, Electrochim. Acta 438 (2023) 141565, https://doi.org/10.1016/j.electacta.2022.141565.

[29] C.M. Branco, S. Sharma, M.M. de Camargo Forte, R. Steinberger-Wilckens, New approaches towards novel composite and multilayer membranes for intermediate temperature-polymer electrolyte fuel cells and direct methanol fuel cells, J. Power Sources 316 (2016) 139–159, https://doi.org/10.1016/j.jpowsour.2016.03.052.

[30] K. Ebert, D. Fritsch, J. Koll, C. Tjahjawiguna, Influence of inorganic fillers on the compaction behaviour of porous polymer based membranes, J. Memb. Sci. 233 (2004) 71–78, https://doi.org/10.1016/j.memsci.2003.12.012.

[31] R. Narducci, E. Sgreccia, P. Knauth, M.L. Di Vona, Anion exchange membranes with 1D, 2D and 3D fillers: a review, Polymers 13 (2021) 3887, https://doi.org/10.3390/polym13223887.
[32] C. Simari, A. Caprì, M.H. Ur Rehman, A. Enotiadis, I. Gatto, V. Baglio, I. Nicotera, Composite anion exchange membranes based on polysulfone and silica nanoscale ionic materials for water electrolyzers, Electrochim. Acta 462 (2023) 142788, https://doi.org/10.1016/j.electacta.2023.142788.
[33] C. Simari, M.H. Ur Rehman, A. Caprì, I. Gatto, V. Baglio, I. Nicotera, High-performance anion exchange membrane water electrolysis by polysulfone grafted with tetramethyl ammonium functionalities, Mater. Today Sustainability 21 (2023) 100297, https://doi.org/10.1016/j.mtsust.2022.100297.
[34] A. Carbone, S.C. Zignani, I. Gatto, S. Trocino, A.S. Aricò, Assessment of the FAA3-50 polymer electrolyte in combination with a $NiMn_2O_4$ anode catalyst for anion exchange membrane water electrolysis, Int. J. Hydrogen Energy 45 (2020) 9285–9292, https://doi.org/10.1016/j.ijhydene.2020.01.150.
[35] J. Guerrero-Contreras, F. Caballero-Briones, Graphene oxide powders with different oxidation degree, prepared by synthesis variations of the Hummers method, Mater. Chem. Phys. 153 (2015) 209–220, https://doi.org/10.1016/j.matchemphys.2015.01.005.
[36] W.S. Hummers, R.E. Offeman, Preparation of graphitic oxide, J. Am. Chem. Soc. 80 (1958) 1339, https://doi.org/10.1021/ja01539a017. –1339.
[37] H. Yu, B. Zhang, C. Bulin, R. Li, R. Xing, High-efficient synthesis of graphene oxide based on improved hummers method, Sci. Rep. 6 (2016) 36143, https://doi.org/10.1038/srep36143.
[38] K.N. Kudin, B. Ozbas, H.C. Schniepp, R.K. Prud'homme, I.A. Aksay, R. Car, Raman spectra of graphite oxide and functionalized graphene sheets, Nano Lett. 8 (2008) 36–41, https://doi.org/10.1021/nl071822y.
[39] V. Scardaci, G. Compagnini, Raman spectroscopy investigation of graphene oxide reduction by laser scribing, J. Carbon Res. 7 (2021) 48, https://doi.org/10.3390/c7020048.
[40] N. Yadav, B. Lochab, A comparative study of graphene oxide: hummers, intermediate and improved method, FlatChem 13 (2019) 40–49, https://doi.org/10.1016/j.flatc.2019.02.001.
[41] K.S. Vasu, B. Chakraborty, S. Sampath, A.K. Sood, Probing top-gated field effect transistor of reduced graphene oxide monolayer made by dielectrophoresis, Solid State Commun. 150 (2010) 1295–1298, https://doi.org/10.1016/j.ssc.2010.05.018.
[42] A. Romero, M.P. Lavin-Lopez, L. Sanchez-Silva, J.L. Valverde, A. Paton-Carrero, Comparative study of different scalable routes to synthesize graphene oxide and reduced graphene oxide, Mater. Chem. Phys. 203 (2018) 284–292, https://doi.org/10.1016/j.matchemphys.2017.10.013.
[43] K. Krishnamoorthy, M. Veerapandian, K. Yun, S.J. Kim, The chemical and structural analysis of graphene oxide with different degrees of oxidation, Carbon 53 (2013) 38–49, https://doi.org/10.1016/j.carbon.2012.10.013.
[44] D. Ion-Ebrasu, B.G. Pollet, S. Caprarescu, A. Chitu, R. Trusca, V. Niculescu, R. Gabor, E. Carcadea, M. Varlam, B.S. Vasile, Graphene inclusion effect on anion-exchange membranes properties for alkaline water electrolyzers, Int. J. Hydrogen Energy 45 (2020) 17057–17066, https://doi.org/10.1016/j.ijhydene.2020.04.195.
[45] F. Farivar, P.Lay Yap, R.U. Karunagaran, D. Losic, Thermogravimetric Analysis (TGA) of graphene materials: effect of particle size of graphene, graphene oxide and graphite on thermal parameters, J. Carbon Res. 7 (2021) 41, https://doi.org/10.3390/c7020041.
[46] A. Caprì, I. Gatto, C. Lo Vecchio, S. Trocino, A. Carbone, V. Baglio, Anion exchange membrane water electrolysis based on nickel ferrite catalysts, ChemElectroChem 10 (2023), https://doi.org/10.1002/celc.202201056.
[47] A. Martinez-Lazaro, A. Caprì, I. Gatto, J. Ledesma-García, N. Rey-Raap, A. Arenillas, F.I. Espinosa-Lagunes, V. Baglio, L.G. Arriaga, $NiFe_2O_4$ hierarchical nanoparticles as electrocatalyst for anion exchange membrane water electrolysis, J. Power Sources 556 (2023) 232417, https://doi.org/10.1016/j.jpowsour.2022.232417.
[48] C. Fujimoto, D.S. Kim, M. Hibbs, D. Wrobleski, Y.S. Kim, Backbone stability of quaternized polyaromatics for alkaline membrane fuel cells, J. Memb. Sci. 423–424 (2012) 438–449, https://doi.org/10.1016/j.memsci.2012.08.045.